AD-A097 131 WASHINGTON UNIV SEATTLE DEPT OF MECHANICAL ENGINEERING F/G 11/6
IMPACTED NOTCH BEND SPECIMEN.(U)
MAR 81 A S KOBAYASHI, M RAMULU, S MALL N00014-76-C-0060
UNCLASSIFIED TR-40 NL

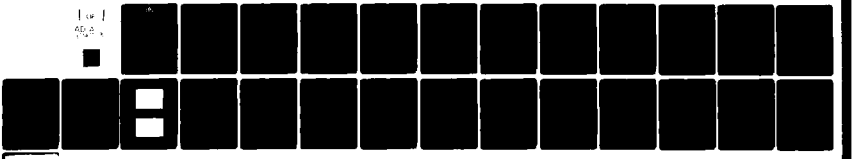

END
DATE FILMED
5-81
DTIC

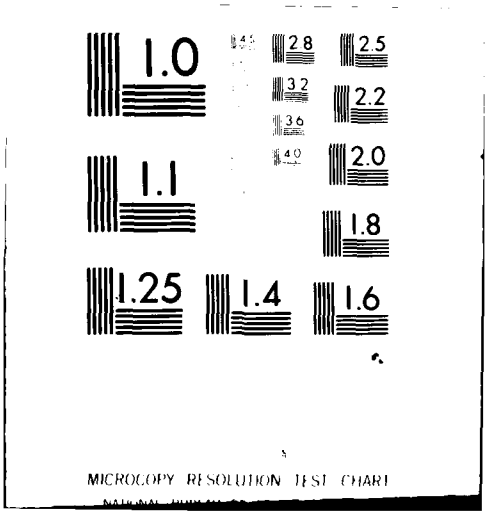
1.0
1.1
1.25
1.4
1.6
1.8
2.0
2.2
2.5
2.8
3.2
3.6
4.0
MICROCOPY RESOLUTION TEST CHART

LEVEL II

12

Office of Naval Research

Contract N00014-76-C-0060 NR 064-478

Technical Report No. 40 TR-

IMPACTED NOTCH BEND SPECIMEN

by

A. S. Kobayashi, M. Ramulu and S. Mall

March 1981

26

The research reported in this technical report was made possible through support extended to the Department of Mechanical Engineering, University of Washington, by the Office of Naval Research under Contract N00014-76-C-0060 NR 064-478. Reporduction in whole or in part is permitted for any purpose of the United States Government.

Department of Mechanical Engineering

College of Engineering

University of Washington

400544

IMPACTED NOTCH BEND SPECIMEN

by

A. S. Kobayashi and M. Ramulu
University of Washington
Department of Mechanical Engineering
Seattle, Washington 98195

and

S. Mall
University of Maine at Orono
Department of Mechanical Engineering
Orono, Maine 94473

ABSTRACT

The proposed method for testing and evaluating data generated by instrumented impact testings of notch bend specimens is evaluated by the experimental and numerical dynamic fracture results obtained in the past. As expected, brittle fracture of the photoelastic, steel and aluminum impacted notch specimens considered in this paper cannot be predicted by the static stress intensity factors at the instant of crack propagation. The fracture energy was only a fraction of the total absorbed energy and was equally unsuitable for dynamic fracture characterization of these specimens. This critical evaluation of the proposed method suggests that despite the enormous correlation studies which justify the use of static analysis, neither the proposed method nor the resultant static stress intensity factor should be used to evaluate the fracture data of impacted notch bend specimens of slightly different configurations.

NOMENCLATURE

a	crack length
B	specimen thickness
c_0	longitudinal bar stress wave velocity
C_{LL}	specimen load-line compliance
E	modulus of elasticity
K_I	mode I stress intensity factor
K_I^{dyn}	mode I dynamic stress intensity factor
K_I^{stat}	mode I static stress intensity factor
K_{Id}	mode I dynamic initiation fracture toughness
P	applied tup load
S	support span of beam
t_f	time to fracture from impact initiation
U	energy
V_0	tup velocity at impact
W	beam depth
δ	load line displacement
σ	normal stress

INTRODUCTION

For over a decade, a variety of instrumented impact testings of notch bend specimens have been used to characterize the fracture resistance of brittle as well as ductile materials. Test specimens for such dynamic fracture testing range from the large notch bend specimens of 38x30x228 cm [1]* to the standard

*Numbers in brackets refer to References at the end of this paper.

Charpy V-notched precracked specimens of 10x10x55 mm [2,3] with test materials ranging from structural steel, to aluminum, titanium, polymers, carbon-epoxy composites and ceramics. The results are normally presented in terms of total absorbed energy (Charpy fracture energy), fracture energy, and dynamic initiation fracture toughness, K_{Id}, all of which are to characterize the material resistance to dynamic loading. Unfortunately, the last two quantities are not directly measurable and the all-inclusive total absorbed energy includes the parasitic kinetic energy for propelling the fractured specimen. As a result, literature is abundant with procedures for interpreting the test results, most of which have involved correlation studies of static analyses of dynamic fracture data of impacted notch bend specimens. While these data have been presented in terms of total absorbed energy, i.e., Charpy fracture energy, in the past, the recent trend is to present the test results in terms of dynamic fracture toughness, K_{Id}. The K_{Id} data and the restrictive conditions under which the data are valid are summarized among others in References [4] and [5]. These empirical procedures are all based on static fracture analysis with restrictive test conditions and data interpretation procedures which assure that the effects of "inertia loading" are excluded. This a priori data filtering excludes the high strain rate loading condition and thus reduces the impact testing to a quasi-static testing condition which in part defeats the original purpose of the test. Despite this uncertainty in its physical characterization, the impacted notch bend specimen is a very popular test specimen because of the simple test procedure involved and its compact specimen size.

With the recent developments in numerical and experimental procedures for analyzing the dynamic responses of cracked structures, some results of numerical [6,7] and experimental [8] dynamic analyses of impacted notch bend specimens are becoming available. One common conclusion which emerges from these dynamic

analyses involving various specimen geometries and materials is that the commonly used static analysis of impact data can lead to erroneous K_{Id} values. The authors have also studied dynamic fracture responses of various impacted notch bend specimens over the past several years [9-12] but did not present these results in terms of the recently proposed method for impact testings of notch bend specimens [5]. The purpose of this paper, thus, is to review these past results in view of recent attempts [13] to relate the results of impacted notch bend specimen to parameters related to dynamic fracture mechanics and in particular, to the dynamic initiation fracture toughness, K_{Id}.

STATIC ANALYSIS OF IMPACTED NOTCH BEND SPECIMEN

Since elastodynamic analysis of an impacted notch bend specimen can, at best, be obtained only by executing large scale finite differences or finite element codes, data evaluation procedures which have evolved to date are based on static analysis of this transient phenomenon. Among the several but similar procedures in use [2-5], the procedure as reported in Reference [5] is briefly described in the following.

The foremost criterion for guaranteeing that specimen inertia oscillation, which refers to the beam vibration of the specimen and which accounts for only part of the dynamic effects, has subsided is the 3τ requirement, where τ is related to the period of the apparent oscillations and can be predicted by [13]

$$\tau = 1.68\ (SWEBC_{LL})^{1/2}/c_0 \tag{1}$$

The specimen compliance, C_{LL}, in equation (1) can be derived from the known specimen deflection in the notch bend beam as [14]

$$C_{LL} = \frac{\delta}{P} = \left(\frac{\delta}{P}\right)_{\text{no crack}} \left[1 + 6\,\frac{W}{S}\,V_2\left(\frac{a}{W}\right)\right] \tag{2}$$

where $\left(\frac{\delta}{P}\right)_{\text{no crack}}$ is the compliance of the uncracked beam and $V_2\left(\frac{a}{W}\right)$, which is the correction factor due to presence of a crack, is represented in a polynomial of $\frac{a}{W}$ in Reference [14].

By adjusting the impact velocity of the tup as well as the specimen geometry, ring down of the impacted specimen is believed to occur when the time to fracture, $t_f > 3\tau$. The dynamic stress intensity can then be computed by using the following static formula [15] of

$$K_I = P_m \frac{S}{BW^{3/2}} f\left(\frac{a}{W}\right) \tag{3}$$

where P_m is the maximum static tup load, and $f\left(\frac{a}{W}\right)$, which is a geometric parameter which corrects for the finite geometry of the beam, is represented by a polynomial $\frac{a}{W}$ in Reference [15].

In addition, complete fracture of the specimen is guaranteed by a conservative requirement that the total available energy at impact, U_0, is larger than three times the energy dissipated at maximum load, or $3U_m$. This requirement also ensures that the tup velocity is not reduced during the fracture initiation event more than 20 percent of its initial impact velocity. In addition, a loading rate in terma of the static stress intensity factor rate of $\dot{K}_I \doteq$ 50 - 500 GPa$\sqrt{m}$/s is computed by the simple formula of:

$$\dot{K}_I = K_I/t_f \tag{4}$$

Although the above static analysis is elastic, impacted notch bend specimens are used to characterize also the fracture resistance of ductile materials, such as A533B steel and low carbon steel. Thus the influence of dynamic plasticity cannot be ignored in practice. Although some attempts have been made to use J for reducing data in the presence of plastic yielding [3,13], such recommended procedures are yet to be established, due to the lack of a definitive static ductile fracture criterion and, needless to mention, a dynamic ductile fracture initiation criterion at this time.

IMPACTED NOTCH BEND PHOTOELECTRIC SPECIMENS

The dynamic stress intensity factors obtained previously, either experimentally by the use of dynamic photoelasticity or by dynamic finite element analysis

of impacted, notch bend photoelastic specimens [10,11], are used to assess the validity of the recommended procedures for dynamic fracture-toughness testing. The two photoelastic specimens of Homalite-100 and polycarbonate used in this comparison are shown in Figure 1. The Homalite-100 and polycarbonate specimens model brittle and somewhat ductile materials, respectively. All cracks were fatigued precracked in these specimens. The specimen geometries which were primarily designed to satisfy the photoelastic requirements are admittedly longer and thinner than the commonly used metallic specimens. Nevertheless, the two-dimensional elastodynamic responses of the photoelastic specimens, with proper care, can be scaled to metallic specimens of smaller dimensions [16,17], and thus these dynamic photoelasticity results were used to dramatize the effectiveness of the recommended procedures. Also shown in Figure 1 is the instrumented tup from which the impact load was obtained.

Figure 2 shows typical tup load traces for the Homalite-100 and polycarbonate specimens. These load traces do not exhibit the oscillating but increasing load responses with time, such as those shown in References [4] and [8], but follow those shown in Reference [5]. These differences could be in part attributed to the higher tup velocities at impact, V_0, used in these series of tests, as shown in Table 1.

Figures 3 and 4 show the static and dynamic stress intensity factors, K_I^{stat} and K_I^{dyn}, up to crack propagation in typical Homalite-100 and polycarbonate specimens, respectively. The static stress intensity factor was computed by substituting the measured instantaneous tup load in equation 3. The dynamic stress intensity factors were either obtained directly by fitting the singular near-field state of stress to the transient isochromatics surrounding the stationary crack tip, or by using a calibrated crack opening displacement obtained from dynamic finite element analysis. Details of the experimental and numerical

procedure used are found in References [15] and [16].

Crack propagation initiated from the fatigued crack tip in four Homalite-100 impacted notch bend specimens within $t_f \doteq 190$ microseconds after initiation of impact, as shown in Figure 3. Equations (1) and (2) yielded a calculated $\tau \doteq 740$ microseconds with a $t_f/\tau = 0.26$ which violates the 3τ impact duration set forth in the recommended procedure. Also notable is the six-fold differences in calculated K_I^{stat} and the actual K_I^{dyn} at crack propagation in Figure 3.

For the seven polycarbonate specimens, the time to fracture is $t_f \doteq 1000$ microseconds, as shown in Figure 4. The calculated $\tau = 980$ microseconds yields a $t_f/\tau \doteq 1$ and is one-third of the specified 3τ limitation. The large differences between the statically computed K_I^{stat} and the actual dynamic K_I^{dyn} are also noted. These differences are in contrast with the reasonable agreements in the Charpy data in the 1τ region shown in Reference [5].

Although the cracks propagated much earlier than the 3τ hold time, the tup load traces for the impacted polycarbonate notch bend specimen in Figure 2 show that the tup load continues to oscillate without abatement after t_f through the duration approaching the 3τ limit. These oscillations are similar to those shown in Reference [8], and thus suggest that K_I^{dyn} would not converge to K_I^{stat} even if initiation of crack propagation was restrained beyond the suggested 3τ limit by lowering the tup velocities at impact in these photoelastic specimens.

Figures 5 and 6 show typical computed energy partitions in impacted Homalite-100 and polycarbonate notch bend specimens. The small percentage of the fracture energy in terms of the total input work at complete specimen fracture shows that the total absorbed energy or the Charpy fracture energy cannot possibly be used to characterize dynamic fracture of Homalite-100. Although the fracture energy occupies about 57 percent of the total absorved energy in the polycarbonate

specimen, for the same reason, would not be an appropriate quantity for dynamic characterization of polycarbonate.

IMPACTED NOTCH BEND STEEL AND ALUMINUM SPECIMENS

A dynamic finite element code was used to determine the increasing K_I^{dyn} leading to K_{Id} at the onset of crack propagation in 25.4 mm thick A533B steel at -18°C and at room temperature, and a 16 mm thick aluminum notch bend specimen [12]. The cracks in the two A533B steel specimens were fatigue-precracked while a mechanically sharpened notch tip of 0.025 mm radius was used in the aluminum specimen. These specimens were instrumented with a 3x3 mm strain gage near the notch tip. The transient strain recorded during impact was then related to an equivalent static stress intensity factor following Loss's procedure [16]. A second strain gage was also located at 1/4 span on the compression edge of the aluminum specimen. Extensive numerical analyses [12] verified that the proximity of the strain gage and the use of instantaneous dynamic strains appeared to compensate for lack of dynamic analysis in Loss's static procedures for computing K_I^{dyn}. The loading rates, $\dot{K}_I^{dyn}$, and the tup velocities at impact, V_0, in these tests are shown in Table 1.

Figures 7 and 8 show the K_I^{stat} and K_I^{dyn} variations in an impacted A533B steel tested at -18°C and room temperature, respectively. With the exception of the fortuitous coincidence of K_I^{stat} and K_I^{dyn} at the initiation of crack propagation in Figure 7, K_I^{dyn} shows no tendency to converge to K_I^{stat} in these figures. The time to fracture, t_f, is about 2τ and 1.2τ for the two A533B speciemns, but the lack of visible convergence of K_I^{dyn} to K_I^{stat} again indicates that K_I^{dyn} will not converge to K_I^{stat} even at the 3τ period.

Figure 9 shows the K_I^{stat} and K_I^{dyn} variations in impacted 6061 aluminum notch bend specimens with $t_f/\tau = 0.81$. Again, the notable differences between K_I^{dyn} and K_I^{stat}, with no trend of abatement, are noted. K_I^{stat} computed from

the 1/4-point strain gage signals, following the procedure described in Reference [5], is not shown in Figure 9. The significant differences in the tup load trace and 1/4-point gage signal, as shown in Figure 11 in Reference [12], would have led to K_I^{stat}, which is appreciably different than the K_I^{dyn} in Figure 9. While the energy partitions of the above three metallic specimens were not determined due to lack of crack velocity measurements during fracture, experiences with other dynamic fracture specimens such as single edged notch (SEN) specimens subjected to uniform loading and fixed end displacement loading [18] show that the total fracture energy dissipated in such specimens would be, at the best, about half of the total input work of the specimen.

CONCLUSIONS AND DISCUSSIONS

Results of our previous experimental and numerical analyses of photoelastic and metallic impacted notch bend specimens, when evaluated in terms of the recommended guidelines for dynamic fracture toughness testing, show that these procedures cannot be extended to the larger specimen configurations used in this analysis.

The credible consistency in the experimental K_{Id} in Reference [5] is based on internal correlations of the dynamic data evaluated statically, which may or may not relate to the actual K_{Id}. The results of the photoelastic test data show that this internal correlation of statically computed K_{Id} breaks down. On the other hand, Figures 3 in References [10] and [11] and Figure 8 in Reference [19] show that the dynamically evaluated K_{Id} are remarkably the same among the four and six Homalite-100 and the seven polycarbonate impacted notch bend specimens tested.

The above comparative study indicates that valid K_{Id} data could be generated through impacted notch bend tests if appropriate dynamic analysis is used. The authors feel that efforts should be expended in developing such a dynamic analysis

procedure rather than in developing restrictive conditions under which static analysis can be used. Conceivably, the long time delay necessary to validate static analysis could obviate the loading rate effect originally sought in these impact tests.

ACKNOWLEDGMENT

The results reported in this paper were obtained through ONR Contract No. 00014-76-C-0600 NR 64-478. The authors with to thank Dr. N. Perrone, ONR, for his support during the course of this investigation.

REFERENCES

1. Loss, F. J. and Pellini, W. S., "Coupling of Fracture Mechanics and Transition Temperature Approaches to Fracture-Safe Design," Practical Fracture Mechanics for Structural Steel, ed. by M. O. Dobson, Chapman and Hall, Ltd., 1969, pp. J1-35.

2. Rolfe, S. T. and Barsom, J. M., Fracture and Fatigue Control in Structures, Applications of Fracture Mechanics, Prentice-Hall, 1977.

3. Instrumented Impact Testing, ASTM STP 563, October 1974.

4. Ireland, D. R., "Procedures and Problems Associated with Reliable Control of the Instrumented Impact Test," Instrumented Impact Testing, ASTM STP 563, October 1974.

5. Server, W. L., Wullaert, R. A. and Sheckherd, J. W., "Evaluation of Current Procedures for Dynamic Fracture-Toughness Testing," Flaw Growth and Fracture, ed. by J. M. Barsom, ASTM STP 631, 1977, pp. 446-461.

6. Norris, D. M., Reaugh, J. E., Moran, B., and Quinones, D. F., "Computer Model for Ductile Fracture: Applications to the Charpy V-Notch Test," EPRI Report No. NP-961, 1979.

7. Kanninen, M. F. Gehlen, P. C., Barnes, C. R., Hoagland, R. G., Hahn, G. T., and Popelar, C. H., "Dynamic Crack Propagation Under Impact Loading," Nonlinear and Dynamic Fracture Mechanics, ed. by N. Perrone, and S. N. Atluri, ASME AMD Vol. 35, 1979, pp. 195-200.

8. Kalthoff, J. F., Bohme, W., Winkler, S. and Klemm, W., "Measurements of Dynamic Stress Intensity Factors in Impacted Bend Specimens," a paper presented at the CSNI International Experts Meeting on Instrumented Precracked Charpy Testing, EPRI, Dec. 1-3, 1980.

9. Kobayashi, A. S. and Urabe, Y., "A Dynamic Photoelastic Analysis of Dynamic Tear Test Specimen," Experimental Mechanics, Vol. 16, No. 5, May 1975, pp. 176-181.

10. Mall, S., Kobayashi, A. S., and Urabe, Y., "Dynamic Photoelastic and Dyanmic Finite Element Analysis of Dynamic-Tear-Test Specimens," Experimental Mechanics, Vol. 18, No. 12, December 1978, pp. 449-456.

11. Mall, S., Kobayashi, A. S., and Urabe, Y., "Dynamic Photoelastic and Dynamic Finite Element Analysis of Polycarbonate Dynamic Tear Test Specimens," Fracture Mechanics, ed. C. W. Smith, ASTM STP 677, August 1979, pp. 498-510.

12. Mall, S., Kobayashi, A. S., and Loss, F. J., "Dynamic Fracture Analysis of Notched Bend Specimens, Crack Arrest Methodology and Applications, ed. M. F. Kanninen and G. T. Hahn, ASTM STP 711, 1980, pp. 70-88.

13. Proceedings of CSNI International Experts Meeting on Instrumented Precracked Charpy Testing, December 1-3, 1980. To be published by EPRI.

14. Tada, H., Paris, P. C., Irwin, G. R., "The Stress Intensity Handbook," Del Research, 1972, p. 2.17.

15. Gross, B., and Srawley, J. W., "Stress Intensity Factors for Three-Point Bend Specimens by Boundary Collocations," NASA TN D-3092, 1965.

16. Kobayashi, A. S., Emery, A. F., and Liaw, B. M., "Dynamic Analysis of Notch Bend Specimens," to be published in the Proceedings of CSNI International Experts Meeting on Instrumented Precracked Charpy Testing, EPRI, 1981.

17. "Structural Integrity of Water Reactor Pressure Boundary Components," Progress Report ending February 1976, F. J. Loss, ed., Naval Research Laboratory Report 8006 (also NRL NUREG.1), 26 August 1976.

18. Kobayashi, A. S., Emery, A. F., and Liaw, B. M., "Dynamic Fracture Characterization of Materials," to be published in Trans. of SMiRT-6, Paris, August 1981.

19. Kobayashi, A. S. and Mall, S., "Dynamic Photoelastic Analysis of Three Dynamic Fracture Specimens," Proceedings of International Conference on Dynamic Fracture Toughness Testing, The Welding Institute, 1976, pp. 259-272.

TABLE 1

SUMMARY OF TEST DATA

	t_f (μsec)	K_{Id} (MPa$\sqrt{m}$)	K_{Ic} (MPa$\sqrt{m}$)	$\dot{K}_I^{dyn}$ (GPa$\sqrt{m}$/sec)	U_0 (Joules)	U_0/U_m (Joules)	V_0 (m/sec)
Homalite-100 (Average of 2 tests at room temperature)	298	.403	.415	3.4	19.2	96.	1.72
Polycarbonate (Average of 2 tests at room temperature)	1070	2.52	3.43	9.7	20.0	8.3	1.73
A533B steel (1 test at 10 C)	424	123	-	460	-	-	2.5
A533B steel (1 test at -18 C)	232	64	-	400	-	-	2.5
6061 aluminum (1 test at room temperature)	140	44	-	500	-	-	8.6

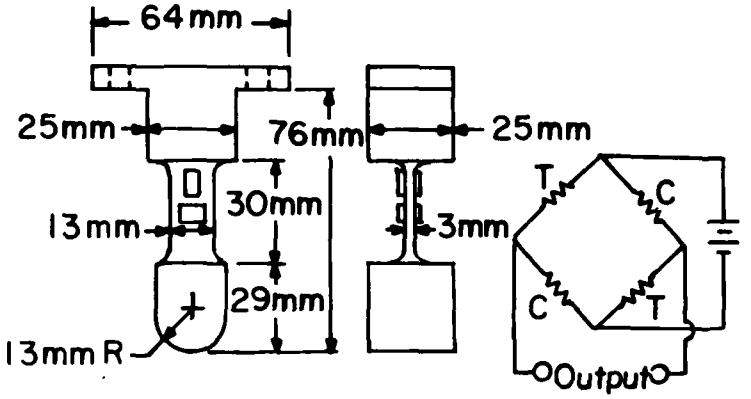

DROP WEIGHT TUP

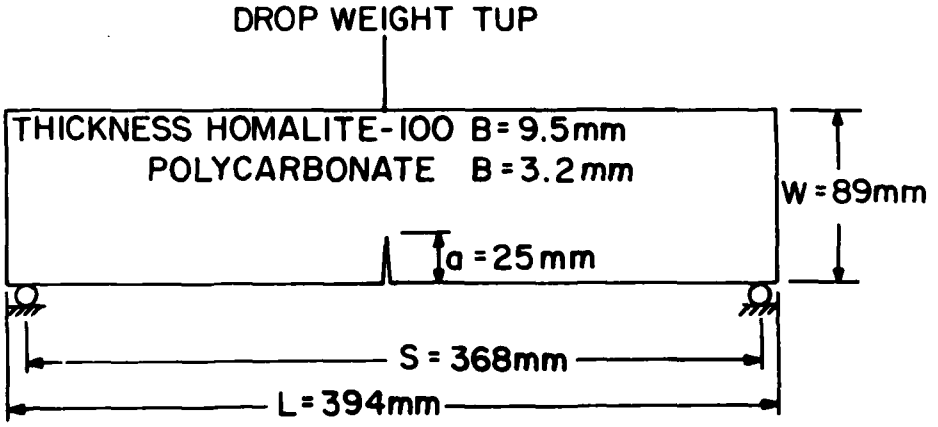

SPECIMEN

FIGURE 1 .HOMALITE-100 AND POLYCARBONATE IMPACTED NOTCH BEND SPECIMEN.

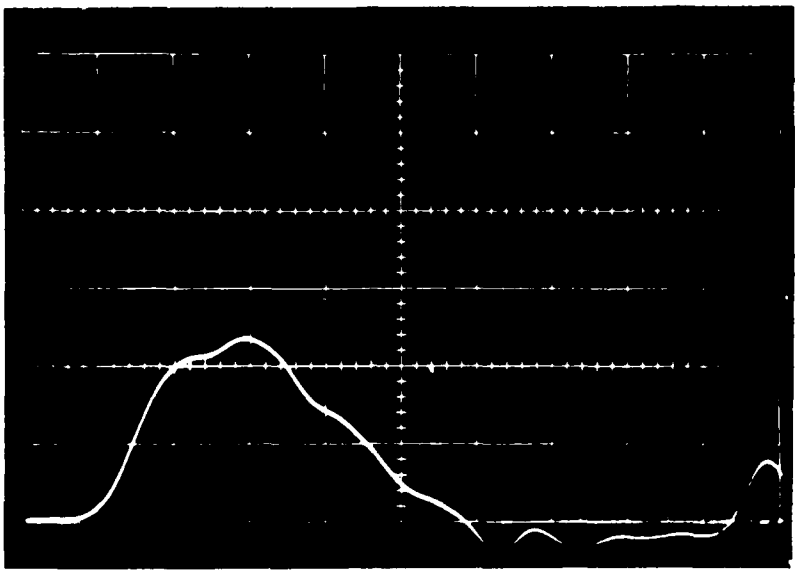

(a) HOMALITE - 100 SPECIMEN
VERTICAL ONE DIVISION = 311 N
HORIZONTAL ONE DIVISION = 0.1 m sec

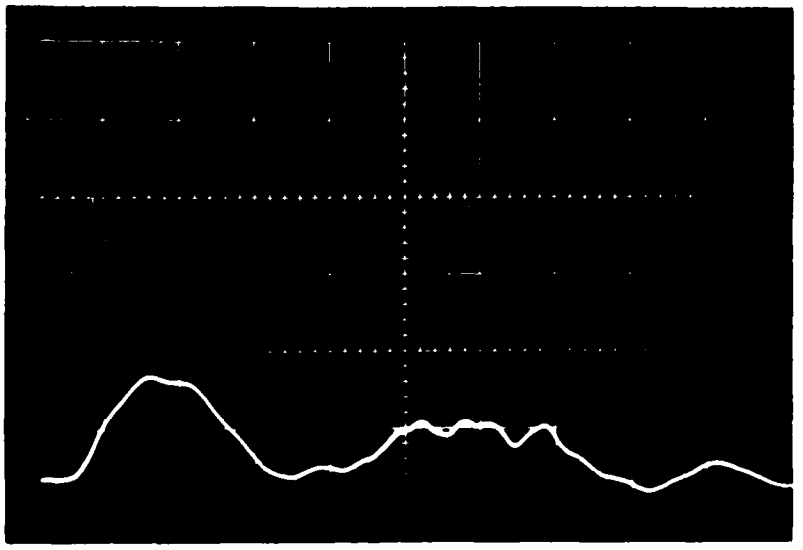

(b) POLYCARBONATE SPECIMEN
VERTICAL ONE DIVISION = 389 N
HORIZONTAL ONE DIVISION = 0.2 m sec

FIGURE 2 . TUP LOAD TRACES FOR IMPACTED HOMALITE - 100 AND POLYCARBONATE SPECIMENS.

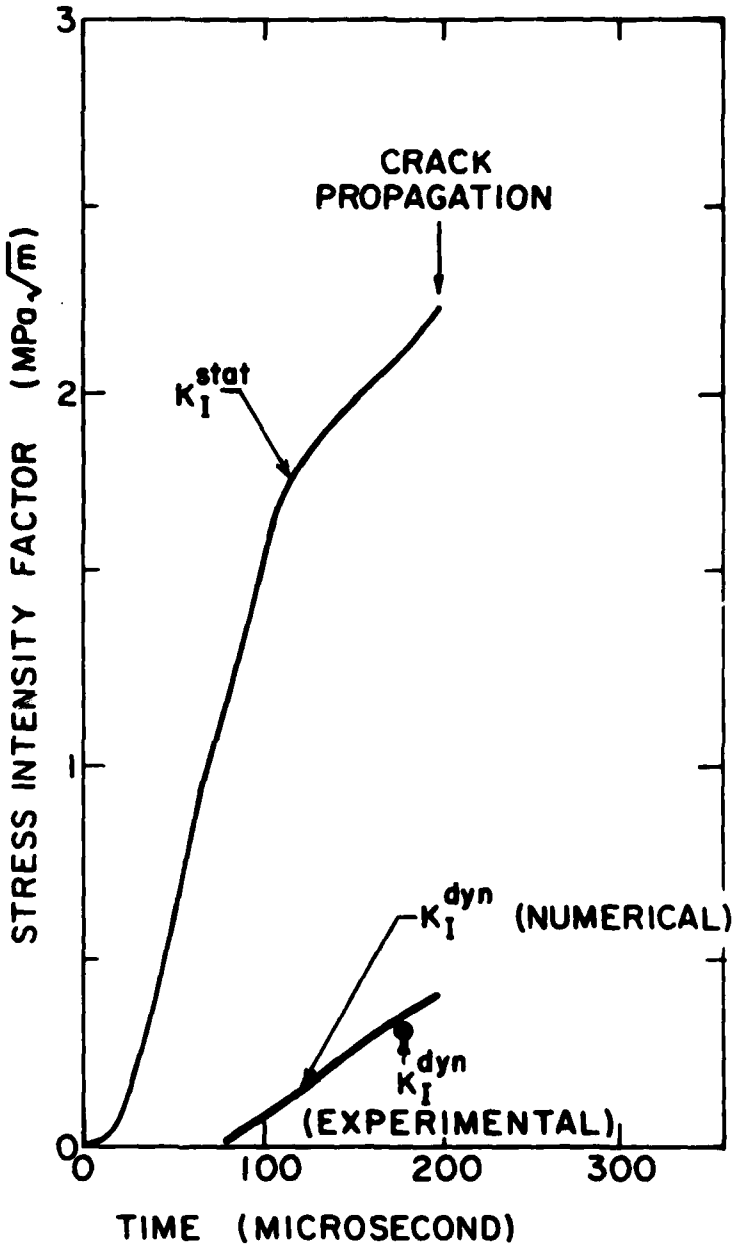

FIGURE 3. STRESS INTENSITY FACTORS OF AN IMPACTED HOMALITE-100 NOTCH BEND SPECIMEN.

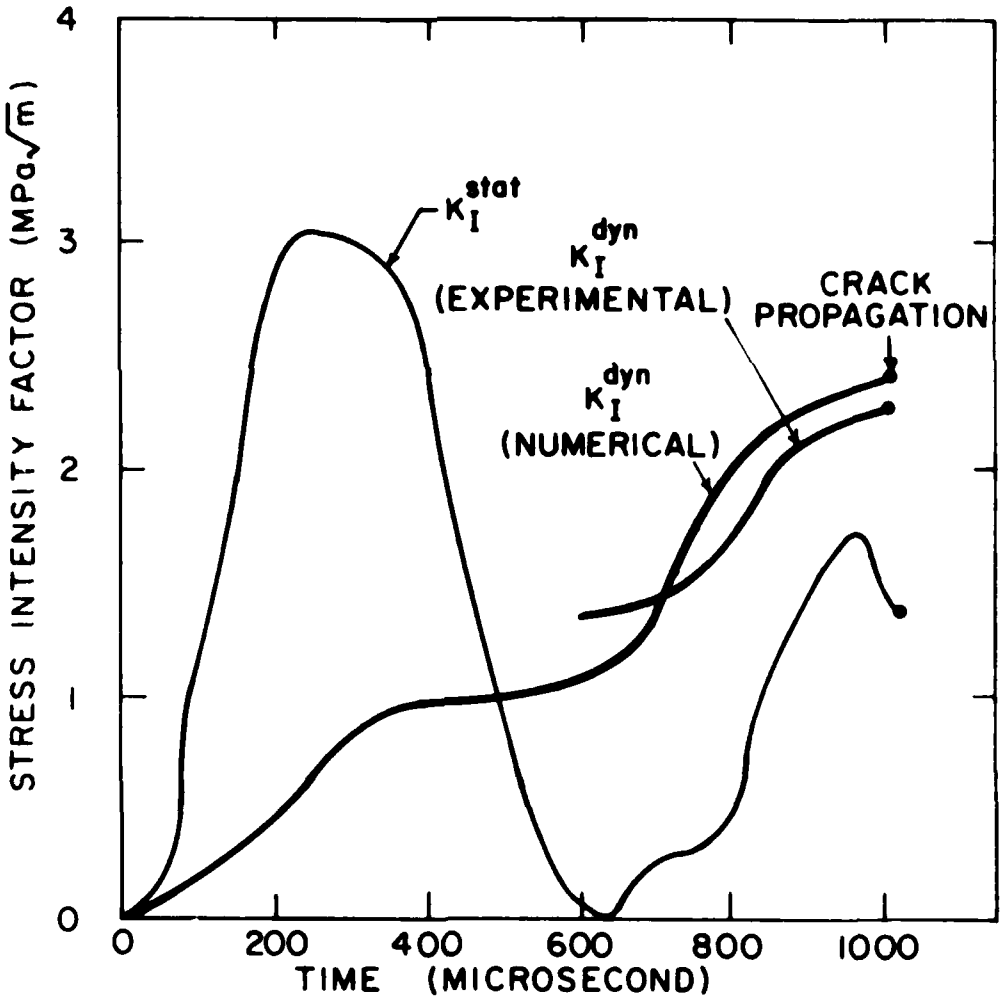

FIGURE 4. STRESS INTENSITY FACTORS OF AN IMPACTED POLYCARBONATE NOTCH BEND SPECIMEN.

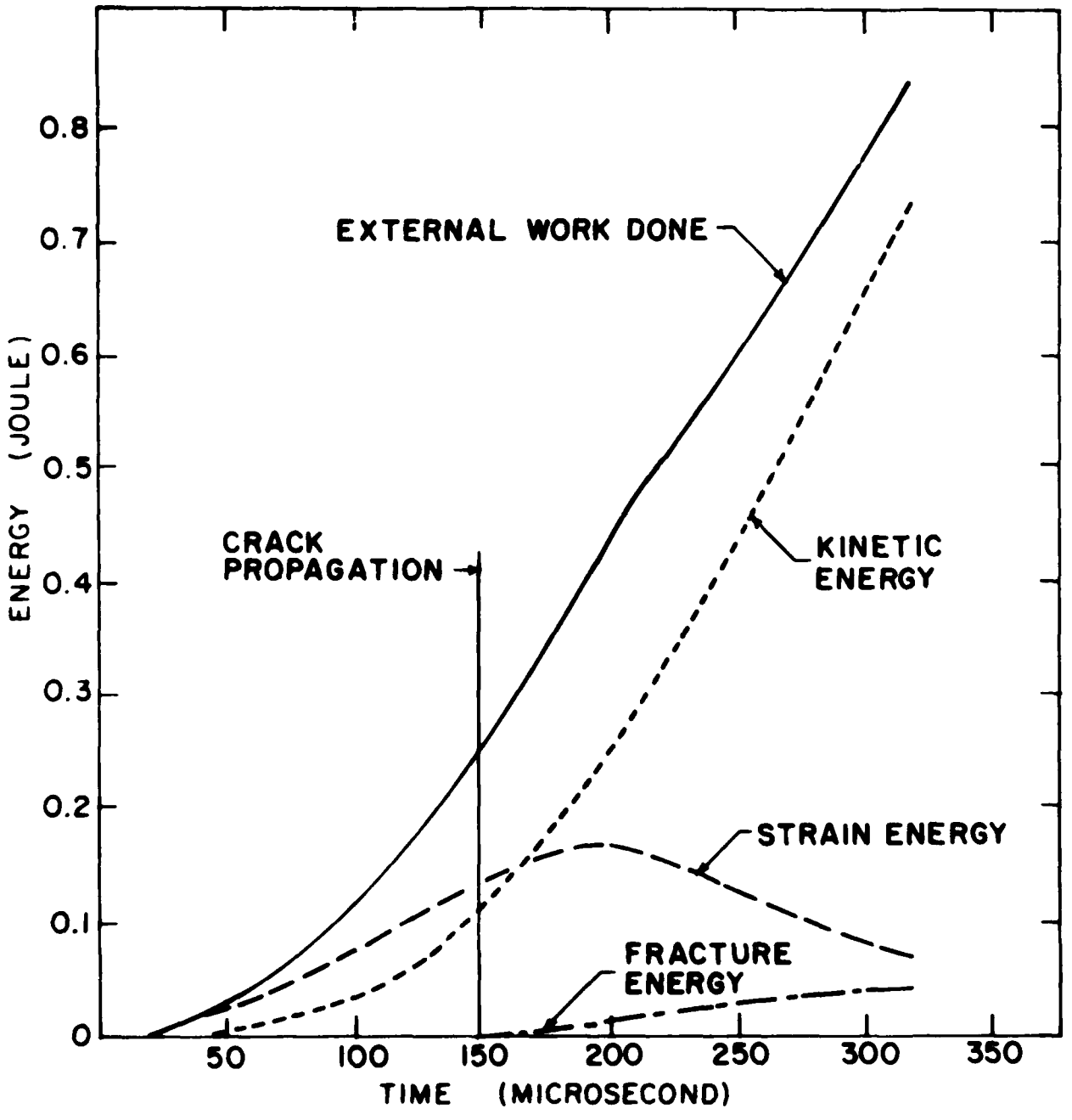

FIGURE 5 . COMPUTED ENERGIES IN IMPACTED HOMOLITE-100 NOTCHED BEND SPECIMEN.

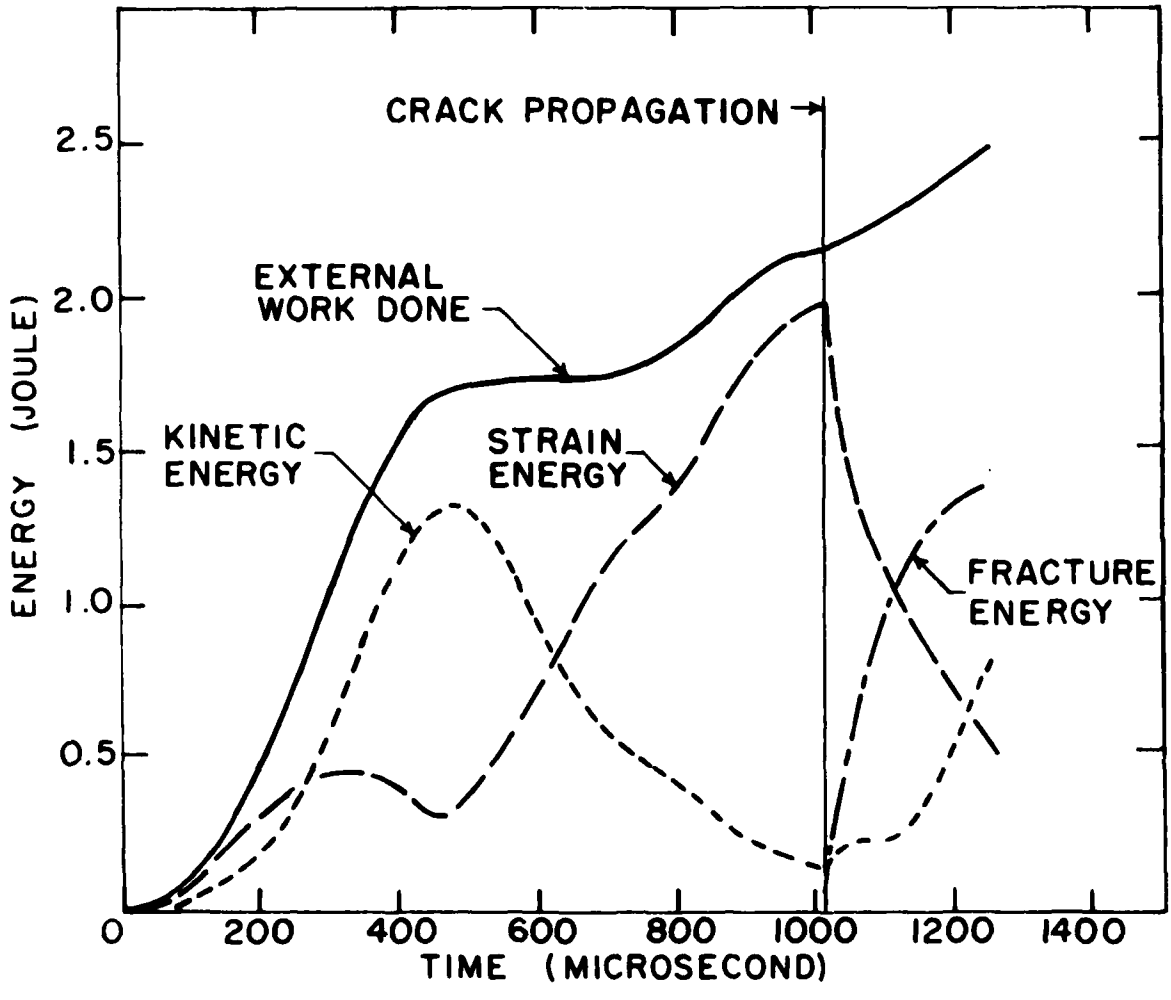

FIGURE 6 . COMPUTED ENERGIES IN IMPACTED POLYCARBONATE NOTCHED BEND SPECIMEN.

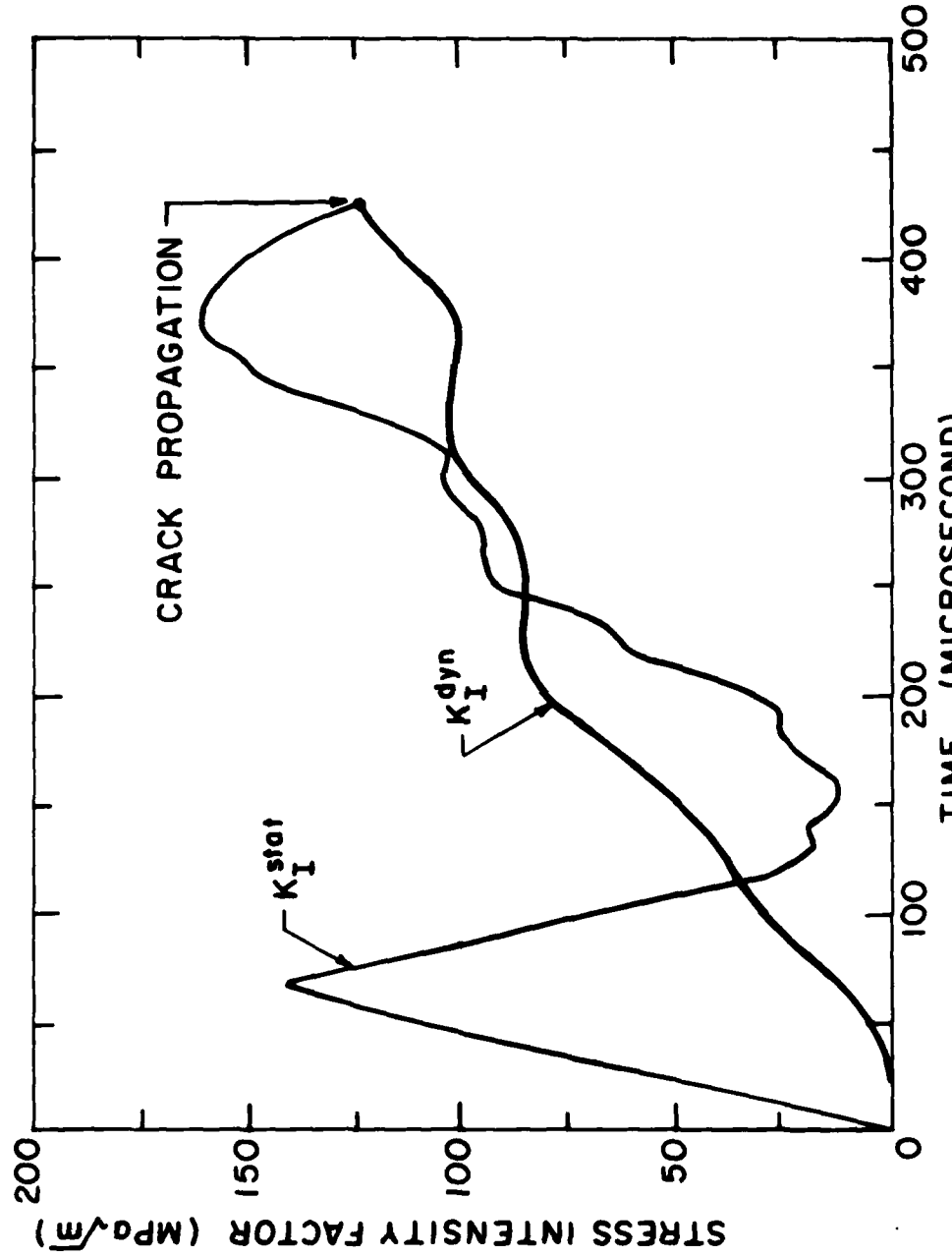

FIGURE 7 .STRESS INTENSITY FACTORS OF AN IMPACTED A533B STEEL NOTCHED BEND SPECIMEN. (L=229, W=51, B=25, a=25mm).

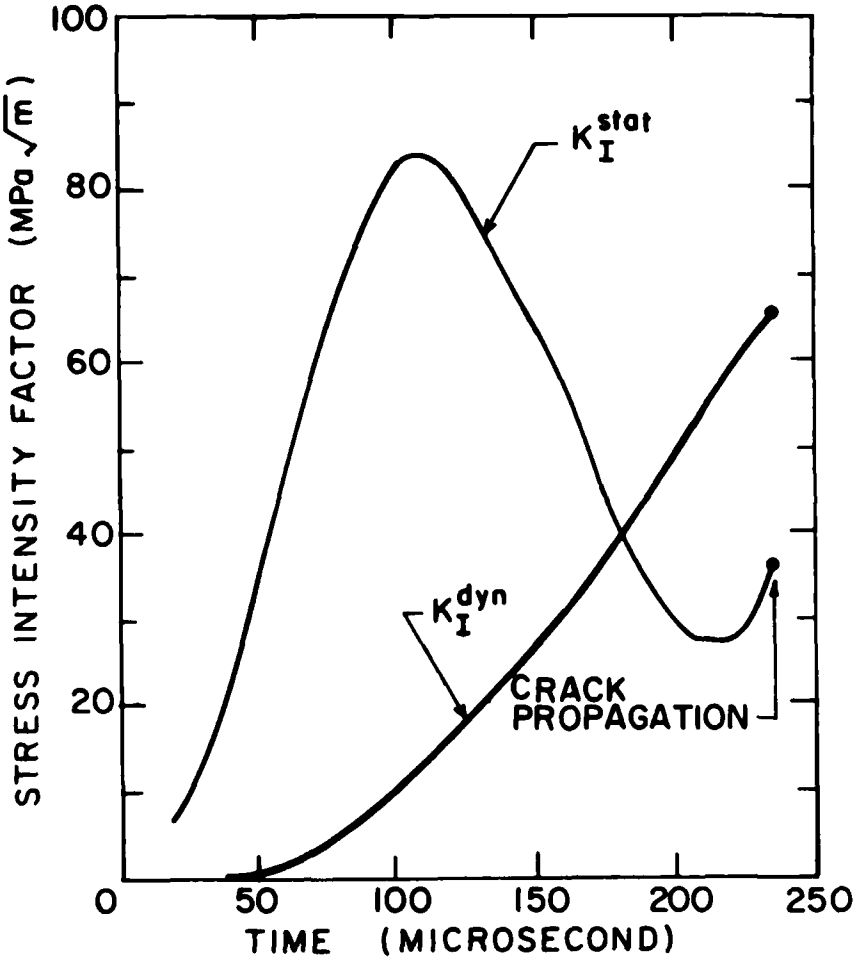

FIGURE 8 . STRESS INTENSITY FACTORS OF AN IMPACTED A533B STEEL NOTCHED BEND SPECIMEN. (L = 229, W = 51, B = 25, a = 25mm)

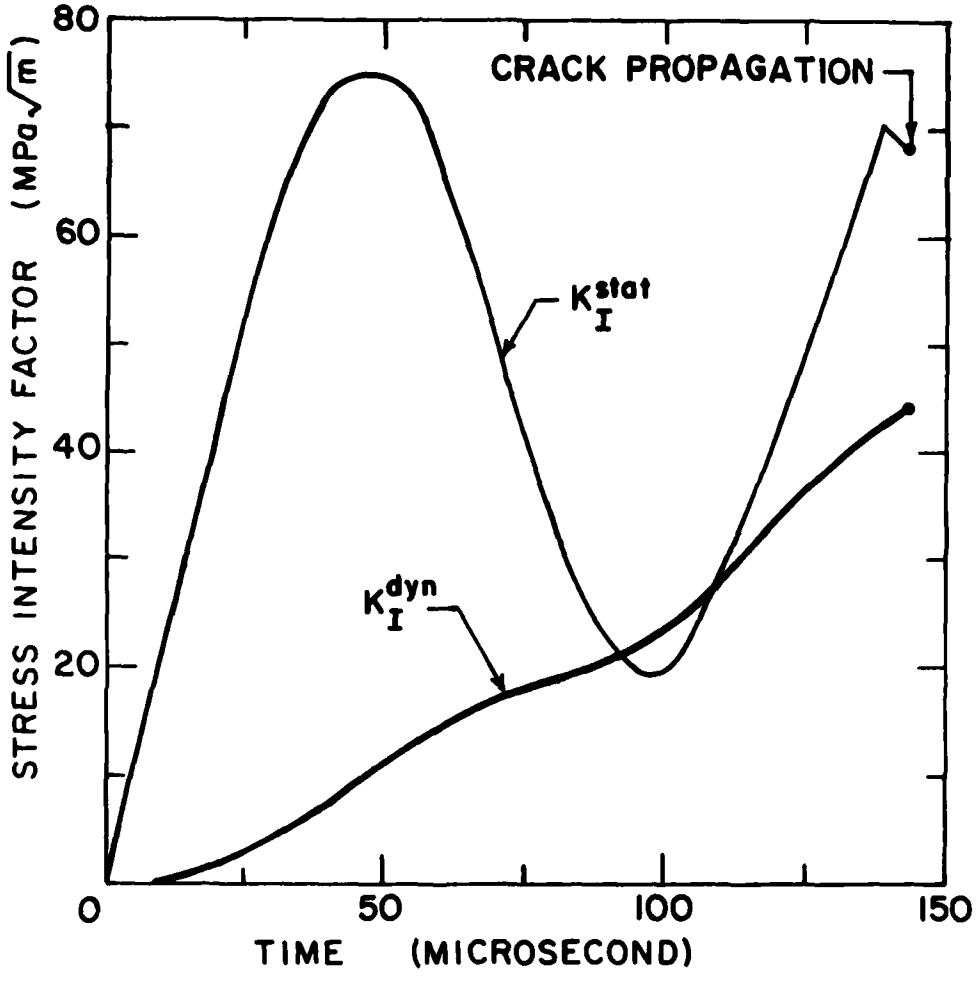

FIGURE 9 . STRESS INTENSITY FACTORS OF AN IMPACTED 6061 ALUMINUM NOTCHED BEND SPECIMEN. (L = 178, W = 41, B = 16, a = 13 mm).

Unclassified

SECURITY CLASSIFICATION OF THIS PAGE (When Data Entered)

REPORT DOCUMENTATION PAGE		READ INSTRUCTIONS BEFORE COMPLETING FORM
1. REPORT NUMBER TR 40	2. GOVT ACCESSION NO. AD-A097 231	3. RECIPIENT'S CATALOG NUMBER
4. TITLE (and Subtitle) Impacted Notch Bend Specimen		5. TYPE OF REPORT & PERIOD COVERED Technical Report
		6. PERFORMING ORG. REPORT NUMBER TR 40
7. AUTHOR(s) A. S. Kobayashi, M. Ramulu and S. Mall		8. CONTRACT OR GRANT NUMBER(s) N00014-76-C-0060
9. PERFORMING ORGANIZATION NAME AND ADDRESS Dept. of Mechanical Engineering FU-10 University of Washington Seattle, WA 98195		10. PROGRAM ELEMENT, PROJECT, TASK AREA & WORK UNIT NUMBERS NR 064-478
11. CONTROLLING OFFICE NAME AND ADDRESS Office of Naval Research Arlington, Virginia 22217		12. REPORT DATE March 1981
		13. NUMBER OF PAGES 19
14. MONITORING AGENCY NAME & ADDRESS(if different from Controlling Office)		15. SECURITY CLASS. (of this report) Unclassified
		15a. DECLASSIFICATION/DOWNGRADING SCHEDULE

16. DISTRIBUTION STATEMENT (of this Report)

Unlimited

17. DISTRIBUTION STATEMENT (of the abstract entered in Block 20, if different from Report)

18. SUPPLEMENTARY NOTES

19. KEY WORDS (Continue on reverse side if necessary and identify by block number)

Dynamic stress intensity factors, dynamic fracture mechanics, Charpy precracked specimens, dynamic finite element analysis, dynamic photoelasticity, impact notch bend specimen

20. ABSTRACT (Continue on reverse side if necessary and identify by block number)

The proposed method for testing and evaluating data generated by instrumented impact testings of notch bend specimens is evaluated by the experimental and numerical dynamic fracture results obtained in the past. As expected, brittle fracture of the photoelastic, steel and aluminum impacted notch specimens considered in this paper cannot be predicted by the static stress intensity factors at the instant of crack propagation. The fracture energy was only a fraction of the total absorbed energy and was equally unsuitable for dynamic fracture

DD FORM 1 JAN 73 1473 EDITION OF 1 NOV 65 IS OBSOLETE
S/N 0102-014-6601

Unclassified

SECURITY CLASSIFICATION OF THIS PAGE (When Data Entered)

20. (cont.)

characterization of these specimens. This critical evaluation of the proposed method suggests that despite the enormous correlation studies which justify the use of static analysis, neither the proposed method nor the resultant static stress intensity factor should be used to evaluate the fracture data of impacted notch bend specimens of slightly different configurations.

Part 1 - Government
Administrative and Liaison Activities

Office of Naval Research
Department of the Navy
Arlington, Virginia 22217
Attn: Code 474 (2)
Code 471
Code 200

Director
Office of Naval Research
Branch Office
666 Summer Street
Boston, Massachusetts 02210

Director
Office of Naval Research
Branch Office
536 South Clark Street
Chicago, Illinois 60605

Director
Office of Naval Research
New York Area Office
715 Broadway - 5th Floor
New York, New York 10003

Director
Office of Naval Research
Branch Office
1030 East Green Street
Pasadena, California 91106

Naval Research Laboratory (6)
Code 2627
Washington, D.C. 20375

Defense Documentation Center (12)
Cameron Station
Alexandria, Virginia 22314

Navy

Undersea Explosion Research Division
Naval Ship Research and Development
Center
Norfolk Naval Shipyard
Portsmouth, Virginia 23709
Attn: Dr. E. Palmer, Code 177

Navy (Con't.)

Naval Research Laboratory
Washington, D.C. 20375
Attn: Code 8400
8410
8430
8440
6300
6390
6380

David W. Taylor Naval Ship Research
and Development Center
Annapolis, Maryland 21402
Attn: Code 2740
28
281

Naval Weapons Center
China Lake, California 93555
Attn: Code 4062
4520

Commanding Officer
Naval Civil Engineering Laboratory
Code L31
Port Hueneme, California 93041

Naval Surface Weapons Center
White Oak
Silver Spring, Maryland 20910
Attn: Code R-10
G-402
K-82

Technical Director
Naval Ocean Systems Center
San Diego, California 92152

Supervisor of Shipbuilding
U.S. Navy
Newport News, Virginia 23607

Navy Underwater Sound
Reference Division
Naval Research Laboratory
P.O. Box 8337
Orlando, Florida 32806

Navy (Con't.)

Chief of Naval Operations
Department of the Navy
Washington, D.C. 20350
Attn: Code OP-098

Strategic Systems Project Office
Department of the Navy
Washington, D.C. 20376
Attn: NSP-200

Naval Air Systems Command
Department of the Navy
Washington, D.C. 20361
Attn: Code 5302 (Aerospace and Structures)
604 (Technical Library)
3208 (Structures)

Naval Air Development Center
Warminster, Pennsylvania 18974
Attn: Aerospace Mechanics
Code 606

U.S. Naval Academy
Engineering Department
Annapolis, Maryland 21402

Naval Facilities Engineering Command
200 Stovall Street
Alexandria, Virginia 22332
Attn: Code 03 (Research and Development)
04B
045
14114 (Technical Library)

Naval Sea Systems Command
Department of the Navy
Washington, D.C. 20362
Attn: Code 05H
312
322
323
05R
32R

Navy (Con't.)

Commander and Director
David W. Taylor Naval Ship
Research and Development Center
Bethesda, Maryland 20084
Attn: Code 042
17
172
173
174
1800
1844
012.2
1900
1901
1945
1960
1962

Naval Underwater Systems Center
Newport, Rhode Island 02840
Attn: Dr. R. Trainor

Naval Surface Weapons Center
Dahlgren Laboratory
Dahlgren, Virginia 22448
Attn: Code G04
G20

Technical Director
Mare Island Naval Shipyard
Vallejo, California 94592

U.S. Naval Postgraduate School
Library
Code 0384
Monterey, California 93940

Webb Institute of Naval Architecture
Attn: Librarian
Crescent Beach Road, Glen Cove
Long Island, New York 11542

Army

Commanding Officer (2)
U.S. Army Research Office
P.O. Box 12211
Research Triangle Park, NC 27709
Attn: Mr. J. J. Murray, CRD-AA-IP

Army (Con't.)

Watervliet Arsenal
MAGGS Research Center
Watervliet, New York 12189
Attn: Director of Research

U.S. Army Materials and Mechanics
Research Center
Watertown, Massachusetts 02172
Attn: Dr. R. Shea, DRXMR-T

U.S. Army Missile Research and
Development Center
Redstone Scientific Information
Center
Chief, Document Section
Redstone Arsenal, Alabama 35809

Army Research and Development
Center
Fort Belvoir, Virginia 22060

NASA

National Aeronautics and Space
Administration
Structures Research Division
Langley Research Center
Langley Station
Hampton, Virginia 23365

National Aeronautics and Space
Administration
Associate Administrator for Advanced
Research and Technology
Washington, D.C. 20546

Air Force

Wright-Patterson Air Force Base
Dayton, Ohio 45433
Attn: AFFDL (FB)
(FBR)
(FBE)
(FBS)
AFML (MBM)

Air Force (Con't.)

Chief Applied Mechanics Group
U.S. Air Force Institute of Technology
Wright-Patterson Air Force Base
Dayton, Ohio 45433

Chief, Civil Engineering Branch
WLRC, Research Division
Air Force Weapons Laboratory
Kirtland Air Force Base
Albuquerque, New Mexico 87117

Air Force Office of Scientific Research
Bolling Air Force Base
Washington, D.C. 20332
Attn: Mechanics Division

Department of the Air Force
Air University Library
Maxwell Air Force Base
Montgomery, Alabama 36112

Other Government Activities

Commandant
Chief, Testing and Development Division
U.S. Coast Guard
1300 E Street, NW.
Washington, D.C. 20226

Technical Director
Marine Corps Development
and Education Command
Quantico, Virginia 22134

Director Defense Research
and Engineering
Technical Library
Room 3C128
The Pentagon
Washington, D.C. 20301

Other Government Activities (Con't)

Dr. M. Gaus
National Science Foundation
Environmental Research Division
Washington, D.C. 20550

Library of Congress
Science and Technology Division
Washington, D.C. 20540

Director
Defense Nuclear Agency
Washington, D.C. 20305
Attn: SPSS

Mr. Jerome Persh
Staff Specialist for Materials
and Structures
OUSDR&E, The Pentagon
Room 3D1089
Washington, D.C. 20301

Chief, Airframe and Equipment Branch
FS-120
Office of Flight Standards
Federal Aviation Agency
Washington, D.C. 20553

National Academy of Sciences
National Research Council
Ship Hull Research Committee
2101 Constitution Avenue
Washington, D.C. 20418
Attn: Mr. A. R. Lytle

National Science Foundation
Engineering Mechanics Section
Division of Engineering
Washington, D.C. 20550

Picatinny Arsenal
Plastics Technical Evaluation Center
Attn: Technical Information Section
Dover, New Jersey 07801

Maritime Administration
Office of Maritime Technology
14th and Constitution Avenue, NW.
Washington, D.C. 20230

PART 2 - Contractors and Other Technical Collaborators

Universities

Dr. J. Tinsley Oden
University of Texas at Austin
345 Engineering Science Building
Austin, Texas 78712

Professor Julius Miklowitz
California Institute of Technology
Division of Engineering
and Applied Sciences
Pasadena, California 91109

Dr. Harold Liebowitz, Dean
School of Engineering and
Applied Science
George Washington University
Washington, D.C. 20052

Professor Eli Sternberg
California Institute of Technology
Division of Engineering and
Applied Sciences
Pasadena, California 91109

Professor Paul M. Naghdi
University of California
Department of Mechanical Engineering
Berkeley, California 94720

Professor A. J. Durelli
Oakland University
School of Engineering
Rochester, Missouri 48063

Professor F. L. DiMaggio
Columbia University
Department of Civil Engineering
New York, New York 10027

Professor Norman Jones
The University of Liverpool
Department of Mechanical Engineering
P. O. Box 147
Brownlow Hill
Liverpool L69 3BX
England

Professor E. J. Skudrzyk
Pennsylvania State University
Applied Research Laboratory
Department of Physics
State College, Pennsylvania 16801

Universities (Con't.)

Professor J. Klosner
Polytechnic Institute of New York
Department of Mechanical and
Aerospace Engineering
333 Jay Street
Brooklyn, New York 11201

Professor R. A. Schapery
Texas A&M University
Department of Civil Engineering
College Station, Texas 77843

Professor Walter D. Pilkey
University of Virginia
Research Laboratories for the
Engineering Sciences and
Applied Sciences
Charlottesville, Virginia 22901

Professor K. D. Willmert
Clarkson College of Technology
Department of Mechanical Engineering
Potsdam, New York 13676

Dr. Walter E. Haisler
Texas A&M University
Aerospace Engineering Department
College Station, Texas 77843

Dr. Hussein A. Kamel
University of Arizona
Department of Aerospace and
Mechanical Engineering
Tucson, Arizona 85721

Dr. S. J. Fenves
Carnegie-Mellon University
Department of Civil Engineering
Schenley Park
Pittsburgh, Pennsylvania 15213

Dr. Ronald L. Huston
Department of Engineering Analysis
University of Cincinnati
Cincinnati, Ohio 45221

Universities (Con't)

Professor G. C. M. Sih
Lehigh University
Institute of Fracture and
Solid Mechanics
Bethlehem, Pennsylvania 18015

Professor Albert S. Kobayashi
University of Washington
Department of Mechanical Engineering
Seattle, Washington 98105

Professor Daniel Frederick
Virginia Polytechnic Institute and
State University
Department of Engineering Mechanics
Blacksburg, Virginia 24061

Professor A. C. Eringen
Princeton University
Department of Aerospace and
Mechanical Sciences
Princeton, New Jersey 08540

Professor E. H. Lee
Stanford University
Division of Engineering Mechanics
Stanford, California 94305

Professor Albert I. King
Wayne State University
Biomechanics Research Center
Detroit, Michigan 48202

Dr. V. R. Hodgson
Wayne State University
School of Medicine
Detroit, Michigan 48202

Dean B. A. Boley
Northwestern University
Department of Civil Engineering
Evanston, Illinois 60201

474:NP:716:lab
78u474-619

Universities (Con't)

Professor P. G. Hodge, Jr.
University of Minnesota
Department of Aerospace Engineering
and Mechanics
Minneapolis, Minnesota 55455

Dr. D. C. Drucker
University of Illinois
Dean of Engineering
Urbana, Illinois 61801

Professor N. M. Newmark
University of Illinois
Department of Civil Engineering
Urbana, Illinois 61803

Professor E. Reissner
University of California, San Diego
Department of Applied Mechanics
La Jolla, California 92037

Professor William A. Nash
University of Massachusetts
Department of Mechanics and
Aerospace Engineering
Amherst, Massachusetts 01002

Professor G. Herrmann
Stanford University
Department of Applied Mechanics
Stanford, California 94305

Professor J. D. Achenbach
Northwest University
Department of Civil Engineering
Evanston, Illinois 60201

Professor S. B. Dong
University of California
Department of Mechanics
Los Angeles, California 90024

Professor Burt Paul
University of Pennsylvania
Towne School of Civil and
Mechanical Engineering
Philadelphia, Pennsylvania 19104

474:NP:716:lab
78u474-619

Universities (Con't)

Professor H. W. Liu
Syracuse University
Department of Chemical Engineering
and Metallurgy
Syracuse, New York 13210

Professor S. Bodner
Technion R&D Foundation
Haifa, Israel

Professor Werner Goldsmith
University of California
Department of Mechanical Engineering
Berkeley, California 94720

Professor R. S. Rivlin
Lehigh University
Center for the Application
of Mathematics
Bethlehem, Pennsylvania 18015

Professor F. A. Cozzarelli
State University of New York at
Buffalo
Division of Interdisciplinary Studies
Karr Parker Engineering Building
Chemistry Road
Buffalo, New York 14214

Professor Joseph L. Rose
Drexel University
Department of Mechanical Engineering
and Mechanics
Philadelphia, Pennsylvania 19104

Professor B. K. Donaldson
University of Maryland
Aerospace Engineering Department
College Park, Maryland 20742

Professor Joseph A. Clark
Catholic University of America
Department of Mechanical Engineering
Washington, D.C. 20064

474:NP:716:lab
78u474-619

Universities (Con't)

Dr. Samuel B. Batdorf
University of California
School of Engineering
and Applied Science
Los Angeles, California 90024

Professor Isaac Fried
Boston University
Department of Mathematics
Boston, Massachusetts 02215

Professor E. Krempl
Rensselaer Polytechnic Institute
Division of Engineering
Engineering Mechanics
Troy, New York 12181

Dr. Jack R. Vinson
University of Delaware
Department of Mechanical and Aerospace
Engineering and the Center for
Composite Materials
Newark, Delaware 19711

Dr. J. Duffy
Brown University
Division of Engineering
Providence, Rhode Island 02912

Dr. J. L. Swedlow
Carnegie-Mellon University
Department of Mechanical Engineering
Pittsburgh, Pennsylvania 15213

Dr. V. K. Varadan
Ohio State University Research Foundation
Department of Engineering Mechanics
Columbus, Ohio 43210

Dr. Z. Hashin
University of Pennsylvania
Department of Metallurgy and
Materials Science
College of Engineering and
Applied Science
Philadelphia, Pennsylvania 19104

Universities (Con't)

Dr. Jackson C. S. Yang
University of Maryland
Department of Mechanical Engineering
College Park, Maryland 20742

Professor T. Y. Chang
University of Akron
Department of Civil Engineering
Akron, Ohio 44325

Professor Charles W. Bert
University of Oklahoma
School of Aerospace, Mechanical,
and Nuclear Engineering
Norman, Oklahoma 73019

Professor Satya N. Atluri
Georgia Institute of Technology
School of Engineering and
Mechanics
Atlanta, Georgia 30332

Professor Graham F. Carey
University of Texas at Austin
Department of Aerospace Engineering
and Engineering Mechanics
Austin, Texas 78712

Dr. S. S. Wang
University of Illinois
Department of Theoretical and
Applied Mechanics
Urbana, Illinois 61801

Industry and Research Institutes

Dr. Norman Hobbs
Kaman AviDyne
Division of Kaman
Sciences Corporation
Burlington, Massachusetts 01803

Argonne National Laboratory
Library Services Department
9700 South Cass Avenue
Argonne, Illinois 60440

474:NP:716:lab
78u474-619

Industry and Research Institutes (Con't)

Dr. M. C. Junger
Cambridge Acoustical Associates
54 Rindge Avenue Extension
Cambridge, Massachusetts 02140

Dr. V. Godino
General Dynamics Corporation
Electric Boat Division
Groton, Connecticut 06340

Dr. J. E. Greenspon
J. G. Engineering Research Associates
3831 Menlo Drive
Baltimore, Maryland 21215

Newport News Shipbuilding and
Dry Dock Company
Library
Newport News, Virginia 23607

Dr. W. F. Bosich
McDonnell Douglas Corporation
5301 Bolsa Avenue
Huntington Beach, California 92647

Dr. R. N. Abramson
Southwest Research Institute
8500 Culebra Road
San Antonio, Texas 78284

Dr. R. C. DeHart
Southwest Research Institute
8500 Culebra Road
San Antonio, Texas 78284

Dr. M. L. Baron
Weidlinger Associates
110 East 59th Street
New York, New York 10022

Dr. T. L. Geers
Lockheed Missiles and Space Company
3251 Hanover Street
Palo Alto, California 94304

Mr. William Caywood
Applied Physics Laboratory
Johns Hopkins Road
Laurel, Maryland 20810

474:NP:716:lab
78u474-619

Industry and Research Institutes (Con't)

Dr. Robert E. Dunham
Pacifica Technology
P.O. Box 148
Del Mar, California 92014

Dr. M. F. Kanninen
Battelle Columbus Laboratories
505 King Avenue
Columbus, Ohio 43201

Dr. A. A. Hochrein
Dandelion Associates, Inc
Springlake Research Road
15110 Frederick Road
Woodbine, Maryland 21797

Dr. James W. Jones
Swanson Service Corporation
P.O. Box 5415
Huntington Beach, California 92646

Dr. Robert E. Nickell
Applied Science and Technology
3344 North Torrey Pines Court
Suite 220
La Jolla, California 92037

Dr. Kevin Thomas
Westinghouse Electric Corp
Advanced Reactors Division
P. O. Box 158
Madison, Pennsylvania 15663


DATE
ILME